Journal of Drug Delivery Science and Technology 53 (2019) 101168

Contents lists available at ScienceDirect

Journal of Drug Delivery Science and Technology

journal homepage: www.elsevier.com/locate/jddst

Disulfide-crosslinked reduction-responsive Prodrug Micelles for On-demand Paclitaxel Release

Zhi Wang[a,1,*], Longbing Ling[b,1], Qing Xia[b], Xinsong Li[b,*]

[a] Department of Plastic Surgery, Peking Union Medical College Hospital, Beijing, 100730, PR China
[b] School of Chemistry and Chemical Engineering, Southeast University, Nanjing, 211189, PR China

ARTICLE INFO

Keywords:
Paclitaxel
Micelles
Reduction-responsiveness
Loading efficiency
Antitumor activity

ABSTRACT

In this report, disulfide-crosslinked paclitaxel (PTX) prodrug micelles were developed through covalently conjugating PTX onto water soluble poly(ethylene glycol)-dihydrolipoic acid (MeO-PEG$_{2k}$-DHLA) via a disulfide linkage and studied their perspectives for chemotherapic antitumor capacity. The polymer-PTX prodrug (MeO-PEG$_{2k}$-SS-PTX), structurally determined by ^{1}H NMR, possessed high PTX content up to 26 wt% and exhibited sharp reduction-responsive behavior. MeO-PEG$_{2k}$-SS-PTX micelles were then subjected to crosslinking by oxidization of thiol (-SH) groups in the core of micellar particles after self-assembly of the amphimictic prodrug. The resultant crosslinked micelles were stable with spherical morphology having the uniform size of 87.67 nm in phosphate buffer (PBS, pH 7.4), as confirmed by transmission electron microscope (TEM) and dynamic light scattering (DLS). The cross-linked micelles based on the redox-sensitive MeO-PEG$_{2k}$-SS-PTX prodrug exhibited an obvious glutathione (GSH)-dependant manner of fast PTX release with appropriate 65.6% in 12 h and 92.6% in 72 h after incubation in PBS medium containing 10 mM GSH. MTT assay together with apoptosis analysis showed that cross-linked MeO-PEG$_{2k}$-SS-PTX micelles worked the higher antitumor activity against MCF-7, A549, BEL-7402 and 4T1 cells, using free PTX as a positive control. More importantly, such micelles were found to hold a longer circulation time in bloodstream and be able to passively targeting accumulate in tumor sites of 4T1-transplanted BALB/c mice model.

1. Introduction

Paclitaxel (PTX), a natural diterpenoid isolated from the bark of Taxus Brevifolia, has displayed substantial anticancer effects induced by stabilizing microtubules, preventing mitosis, and prompting cellular apoptosis [1,2]. As the first-line antitumor drug, PTX has been broadly applied in the medication of various solid tumors, such as breast, ovarian, and prostate cancers [3–5]. In addition, PTX has also been realized to be successful in combating versus lung, non-small cell lung carcinoma and AIDS-related Kaposi's sarcoma [6,7]. However, its applications in cancer chemotherapy are hampered by its poor solubility, prominent toxicity, lower bioavailability and non-specificity [8–10]. A formulation of PTX containing CremophorEL (CrEL) under the tradename Taxol® has been permitted by U.S. Food and Drug Administration to improve its solubility and to cure patients having diverse malignancies as mentioned above [10]. Unfortunately, severe side effects were observed in Taxol®, such as hypersensitivity, nephrotoxicity and peripheral neuropathy [11–13]. A novel PTX formulation (Abraxane®) devoid of CrEL [14,15] has been introduced to overcome these limitations of Taxol®, but it also possesses many inadequacies, including high-cost, short half-life and feeble antitumor effect compared to Taxol®. Therefore, alternative formulations of the currently available commercialized PTX are highly required in chemotherapeutic treatment.

To meet the challenge of associated toxicity of the commercial PTX formulation, intelligent polymer-based drug delivery systems (DDS) of PTX lacking CrEL as an additive have been developed to overcome such kind of limitations [16–19]. Except for the lower toxic effects, polymeric formulations of PTX have various advantages over the standard current chemotherapy, including increased aqueous solubility of conjugated drugs, along with nanoscaled characteristics, which enables their effective tumor-targeted delivery into the tumor site via enhanced permeability and retention (EPR) effect [20–22]. Recently, polymeric prodrugs attract much attention in the community of drug delivery [23]. Conjugation of the antitumor drugs with polymeric backbones like polysaccharide (TPS) [24] or polyethylene glycol (PEG) [25–27], potentially escape the reticuloendothelial system (RES) in normal cells/

* Corresponding authors.
E-mail addresses: wangzh@pumch.cn (Z. Wang), lixs@seu.edu.cn (X. Li).
[1] These authors contributed equally to this work.

https://doi.org/10.1016/j.jddst.2019.101168
Received 15 April 2019; Received in revised form 18 July 2019; Accepted 18 July 2019
Available online 19 July 2019
1773-2247/

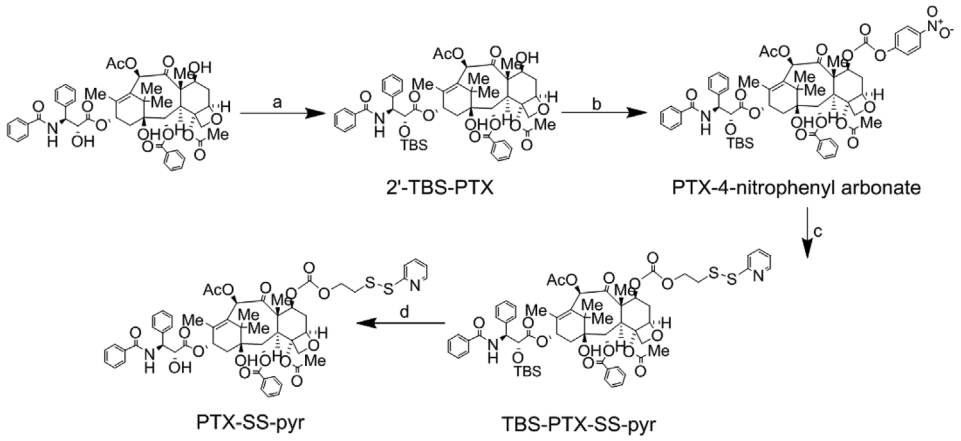

Scheme 1. The detailed synthetic pathway for disulfide-linked PTX–SS–Pyr conjugate. Regents and conditions: (a) imidazole, TBDMSCl, DMF, r.t., 24 h; (b) p-nitrophenyl chloroformate, DMAP, CH_2Cl_2, r.t., 12 h; (c) 2-(pyridin-2-yldisulfanyl)ethanol, CHCl3, 70 °C, 12 h; (d) TBAF, THF, r.t., 2 h.

tissues, thereby minimizing the drugs associated adverse side effects. Such modification of PTX into nanoparticles also improves the pharmacokinetic profile of PTX by increasing its half-life in bloodstream and tumor accumulation. Along with the mentioned polymeric conjugates, several other polymer-based nano-formulation approaches to deliver PTX have been explored, including PTX-loaded micelles, emulsion [28] and cyclodextrins modified complexes [29,30], however only few of them was approved by the Food and Drug Administration (FDA). This is possibly because of their lower drug loading, batch-to-batch dissimilarities in its bio-physicochemical characteristics, inadequate biocompatibility, higher toxicity, and poor *in vivo* instability of these nanosystems [31,32].

The *in vivo* instability of the conventional micellar nanomedicines is mainly linked to their early crumbling in the systemic circulation. Dilution in the blood together with interactions of the micellar building blocks with plasma proteins cause this premature disintegration, that actively transfers the micellar equilibrium to the unimer status after intravenous administration [33,34]. This phenomenon results in the trivial developments in the circulation periods, targeted accumulation at tumor site and therapeutic efficiency of the substantial number of pre-clinically applied micellar nanomedicines [35]. Introduction of crosslinking is an easy and straightforward approach to decline the premature disintegration of polymer-based nanosystems to ensure extended circulation in bloodstream, as well as effective EPR-facilitated targeted accumulation. Using this strategy, the assembly of unimers is further stabilized through the construction of crosslinks (covalent, hydrogen bonding or π-π stacking) [36–38] both in the core or corona to develop robust cross-linked micellar systems. However, the physically entrapped drugs rapidly leaked out from the micellar core, nearly irrespective of core-crosslinking, thereby quickly eliminated from the blood circulation. And the physically entrapped drug candidates released from the micellar systems in a non-controlled fashion, which is inadequate for assuring sustained and tailored release kinetics.

One way to counteract such premature diffusion or controlled the release of the incorporated drugs from the micellar systems at higher level, is to develop covalently co-crosslinked drug micelles employing various biodegradable linkers. Covalently cross-linking significantly improved the pharmacokinetic properties of polymeric micelles versus the physically (non-covalently) encapsulated drugs [39,40]. Specifically, the covalently attached stimuli-responsive core-cross-linked micelles containing disulfide (–SS–) linkages could not only guarantee the retaining of drug molecules in the micelles throughout the systemic circulation, but also ensure its effective release after accumulating at the target site [41]. Such core cross-linked micelles uphold higher stability in bloodstream/extracellular environment with lower glutathione(GSH) level [41], but could quickly break the –SS– bonds to release the payload under extremely reductive milieu in tumor. In this context, Page and coworkers developed camptothecin (CPT)-conjugated cross-linked micelles containing –SS– linkage, which demonstrated potentially declined the premature diffusion of CPT from the micellar core, when compared with physically entrapped CPT. The presence of –SS– bonds in the prodrug micelles facilitated CPT release under reducing environment, which potentially induced the deaths of MCF-7 cells.

The rationale of the current study is to design stimuli responsive core-cross linked micelles of covalently conjugated PTX having a –SS– linker and to explore their stability, sustained release, antitumor efficacy, as well as provide an evidence of their prolonged circulation in bloodstream. For the purpose, core-cross linked micelles based on the PTX-conjugated MeO-PEG_{2k}-DHLA prodrug (MeO-PEG_{2k}-SS-PTX) was developed. In the designing of this prodrug, pyridyldithio-modified PTX was covalently conjugated with MeO-PEG_{2k}-DHLA block through a cleavable –SS– bond and self-assembled into cross-linked micelles by oxidization. With the PEGylated shell and disulfide crosslinking in the core, these micelles exhibited substantial stability in physiological condition but quickly liberate PTX at the rich GSH milieu of tumor sites due to disulfide cleavage (Scheme 3). Besides, *in vitro* cytotoxicity, apoptosis analysis and *in vivo* pharmacokinetics of cross-linked micelles were investigated in detail.

2. Materials and methods

2.1. Materials

Paclitaxel (PTX) with the purity of 98.5% was obtained from Aikon Biopharmaceutical R&D Co., Ltd. Nanjing, China. Poly(ethylene glycol) methyl ether (MeO-PEG-OH, Mw 2000 Da), succinic anhydride (SA), serinol, lipoic acid (LA) and sodium borohydride ($NaBH_4$) were purchased from Sinopharm Chemical Reagent Co., Ltd. Shanghai, China. 4-(dimethylamino) pyridine (DMAP), p-nitrophenyl chloroformate, sodium dodecyl sulfate (SDS), imidazole, tert-butyldimethylsilyl chloride (TBDMSCl), dicyclohexylcarbodiimide (DCC) and 2,2′-dithiodipyridine were purchased from J&K Scientific Ltd. Shanghai, China. Cell culture reagents including completed RPMI-1640 medium, fetal bovine serum (FBS) and trypsin-EDTA were purchased from Key Gen Biotech Co., Ltd. Nanjing, China. All other chemicals and reagents were analytical grade and used without further purification.

MCF-7 cells, A549 cells and BEL-7402 cells were provided by Public Health Institute of Southeast University. Cells were incubated in completed RPMI-1640 medium supplemented with 10% FBS and maintained in a humidified atmosphere of 5% CO_2 at 37 °C.

Female BALB/c mice (5-week-old, 18–20 g) were acquired from

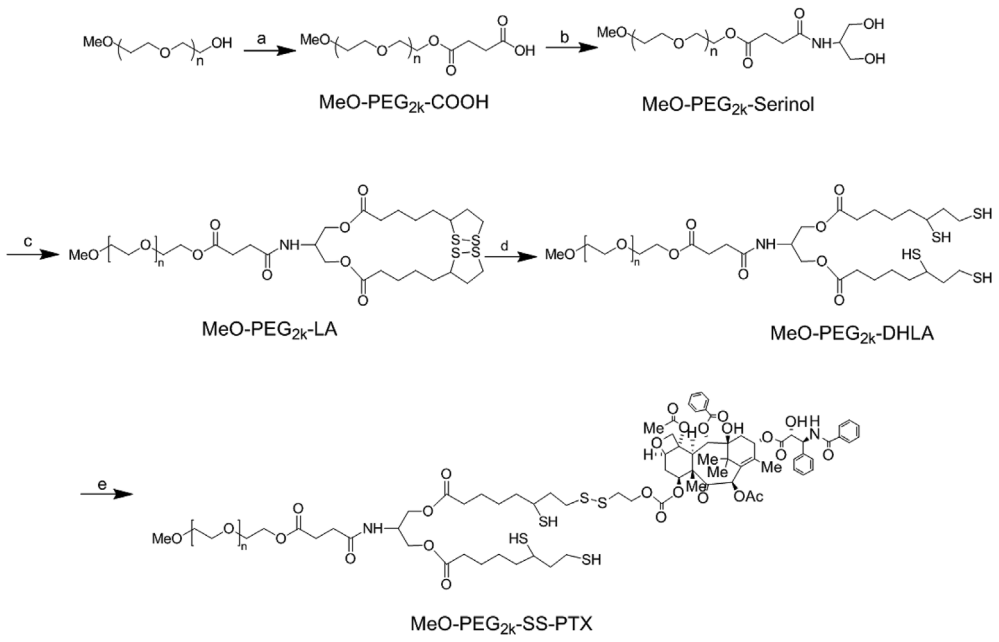

Scheme 2. The detailed synthetic pathway for disulfide-linked MeO-PEG_{2k}-SS-PTX prodrug. Regents and conditions: (a) SA, DMAP, Et_3N, CH_2Cl_2, reflux, 12 h; (b) serinol, DCC/HOBt, CH_2Cl_2, r.t., 8 h; (c) LA, DCC/DMAP, DMF, r.t., 12 h; (d) $NaBH_4$, MeOH/H_2O, 0 °C, 4 h; (e) PTX–SS–Pyr, Et_3N, DMF, r.t., 12 h.

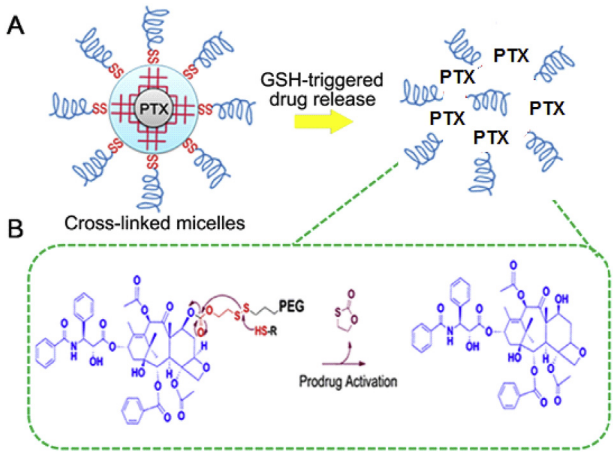

Scheme 3. Schematic illustration of GSH-triggered PTX release (A) and the proposed reduction-responsive mechanism (B) from cross-linked MeO-PEG_{2k}-SS-PTX micelles *in vitro*.

Animal Core Facility of Nanjing Medical University and held under sterile conditions. All animal's experiments were strictly conducted in accordance with the guidelines set by the Institutional Animal Care and Use Committee of Southeast University.

2.2. Synthesis of PTX–SS–Pyr conjugate

Scheme 1 gives the synthetic pathway of disulfide-linked PTX–SS–Pyr conjugate using a four-step conjugation approach. The synthesis and structural characterizations are detailed as follows:

1st step: 2′-TBS-PTX that 2′-OH of reactive PTX was protected by TBDMSCl agent was synthesized as we previously reported [42]. The final yield of 2′-TBS-PTX is appropriate 98.6%.

2nd step: To a mixture of 2′-TBS-PTX (1.5 g, 1.55 mmol) and 4-nitrophenyl chloroformate (0.62 g, 3.12 mmol) dissolved in 20 mL of dried dichloromethane at 0 °C, DMAP (1.14 g, 9.30 mmol) was dropwisely added and stirred for overnight. After that, the mixture was washed by 0.1 M HCl (150 mL), dried by anhydrous Na_2SO_4 and solvent was removed in vacuo. PTX-4-nitrophenyl carbonate was obtained as a white solid (1.52 g, yield 85.7%) after purification via silica gel column chromatography (EtOAc:Hexane 1:2). MS *m/z*: calculated for $C_{60}H_{68}N_2O_{18}Si$ $[M+Na]^+$, 1155.42; found 1155.41 $[M+Na]^+$.

3rd step: PTX-4-nitrophenyl carbonate (1.5 g, 1.33 mmol), 2-(pyridin-2-yldisulfanyl) ethanol (0.49 g, 2.66 mmol) and DMAP (0.46 g, 3.99 mmol) dissolved in 40 mL of anhydrous chloroform, reflux at 80 °C for 12 h. After cooled, washed with distilled water (100 mL) and dried by Na_2SO_4, removal of solvents and purified using silica column chromatography (EtOAc:Hexane 1:2) to obtain the product of TBS-PTX–SS–Pyr as a white solid (1.26 g, yield 80.3%). MS *m/z*: calculated for $C_{61}H_{72}N_2O_{16}S_2Si$ $[M+Na]^+$, 1203.41; found 1203.39 $[M+Na]^+$.

4th step: The acquired TBS-PTX–SS–Pyr was further subjected to deprotection of TBS group by solution to achieve the final product of PTX–SS–Pyr. Briefly, to a solution of TBS-PTX–SS–Pyr (1.18 g, 1.0 mmol) in 5 mL of THF, μL of 1 M tetra-butylammonium fluoride (TBAF) in THF was added and allowed to maintain at r.t. for 2 h. Removal of solvent followed by purification on silica column (1:1 EtOAc:hexane) provided PTX–SS–Pyr as a white solid (1.07 g, yield 73.5%). ^{1}H NMR (500 MHz, $CDCl_3$): δ 1.19–1.24 (m, 6H, –CH_3), 1.77 (s, 3H, –CH_3), 1.84 (s, 3H, –CH_3), 2.30 (d, *J* = 9.7 Hz, 3H, –$COCH_3$), 3.06 (d, *J* = 6.9 Hz, 2H, –CH_2-), 3.84 (d, *J* = 6.7 Hz, 1H, H3), 4.08 (ddd, *J* = 21.4, 11.4, 5.4 Hz, 2H, –CH_2-), 4.24 (d, *J* = 8.3 Hz, 2H, H20), 4.36 (m, 2H, H19), 4.73 (m, 1H, H7), 4.88 (d, *J* = 7.9 Hz, 1H, H5), 5.37 (m, 1H, H3'), 5.60 (d, *J* = 6.8 Hz, 1H, H11), 5.72 (m, 2H, H2), 6.15–6.24 (m, 4H, H10, H13), 7.02–8.49 (m, –C_6H_6) ppm. ^{13}C NMR (500 MHz, $CDCl_3$): δ 13.63, 19.66, 21.53, 25.55, 32.36, 34.53, 35.72, 42.22, 45.94, 53.93, 55.12, 64.93, 71.23, 74.24, 74.60, 75.40, 75.79, 76.00, 76.22, 77.52, 79.97, 82.80, 114.62, 118.79, 125.12, 127.36, 127.73, 127.99, 129.14, 131.01, 132.07, 132.57, 132.78, 136.16, 136.93, 139.46, 148.56, 152.89, 165.83, 166.16, 201.68 ppm. MS *m/z*: calculated for $C_{55}H_{58}N_2O_{16}S_2$ $[M+Na]^+$, 1098.32; found 1098.39 $[M+Na]^+$.

2.3. Synthesis of MeO-PEG_{2k}-SS-PTX prodrug

MeO-PEG_{2k}-SS-PTX prodrug with a disulfide linkage was synthesized by a five-step facial conjugation method as illustrated in Scheme 2. The carboxyl terminated PEG monomethyl ether (MeO-PEG_{2k}-COOH) was first synthesized with SA (4 eq.) and DMAP (1 eq.) in pyridine through an esterification reaction [43]. After that, serinol (3

eq.) was attached to the MeO-PEG_{2k}-COOH (1 eq.) using DCC (2 eq.)/HOBt (2 eq.) as the coupling agents in chloroform overnight. The polymer of MeO-PEG_{2k}-Serinol was precipitated in ice-cold ether three times and concentrated under vacuum. Furthermore, MeO-PEG_{2k}-Serinol, lipoic acid (LA), DCC and DMAP with the molar ratio of 1:4:4.5:1 were dissolved in anhydrous DMF and left to proceed at r.t. for 24 h. The solution was filter and isolated as a light yellow solid of MeO-PEG_{2k}-LA polymer after precipitation in ice-cold ether. Afterward, MeO-PEG_{2k}-LA was completely reduced to MeO-PEG_{2k}-DHLA in the free thiol form (-SH) and the above-acquired PTX–SS–Pyr conjugate (4 eq.) was finally coupled onto the host polymer of MeO-PEG_{2k}-DHLA (1 eq.) in triethylamine (Et_3N) through a thiol–disulfide exchange reaction. The reactants were stirred at room temperature for 12 h. MeO-PEG_{2k}-SS-PTX prodrug was obtained by extensive dialysis (MWCO 1000) against distilled water followed by lyophilization.

2.4. Preparation and characterization of cross-linked MeO-PEG_{2k}-SS-PTX micelles

Cross-linked MeO-PEG_{2k}-SS-PTX micelles were fabricated by a DMF dissolution of polymer MeO-PEG_{2k}-SS-PTX prodrug dropwise into the phosphate buffer saline (PBS, pH 7.4) under stirring at room temperature. To facilitate the intermolecular disulfide (–SS–) crosslinking, the solution was oxidized by purging air continuously for 24 h. The loss of free thiol (-SH) groups was checked using Ellman's test [44]. The micelles obtained were then filter thrice via a syringe filter (0.11 μm, Corning Incorporated, NY) and sonicated for 20 min, which were used for the following characterization at a reserved concentration of 1 mg PTX/mL.

Critical micelle concentration (CMC) of cross-linked MeO-PEG_{2k}-SS-PTX micelles was determined by a dye solubilization method using pyrene. Sample suspensions of pyrene in acetone were prepared and evaporated the solvent to a final concentration of pyrene at 6×10^{-7} M. After that, different concentrations (3 mL) of MeO-PEG_{2k}-SS-PTX prodrug were added to each tube for another 24 h equilibration between micelles and pyrene. The fluorescence emission spectra were measured at the excitation wavelength of 335 nm by a LS-50B spectrometer (Perkin Elmer, MA, USA). The intensity ratio of I_3/I_1 (third and first highest energy bands) was plotted the logarithm of concentrations (Log C) to obtain CMC value.

The amount of conjugated PTX in the micelles was determined by HPLC instrument (Agilent, MA, USA) after releasing PTX from MeO-PEG_{2k}-SS-PTX micelles by adding excessive GSH. The loading content was calculated according to the standard calibration curve that is attained between HPLC area values and different concentrations of PTX drug in methanol. The definition of drug loading capacity (DLC) is presented as the maximum PTX content accomplished by the micelles, while the drug conjugation efficiency (CE) is defined as the ratio of weight of conjugated drug to the initial drug input.

The size and size distribution of MeO-PEG_{2k}-SS-PTX micelles after crosslinking were monitored at 25 °C by dynamic light scattering (DLS, Malvern, Worchestershire, UK). 1 mg/mL of micellar solution were filtered through a 0.22 μm syringe filter before test and measurements were performed by the Zetasizer Nano-ZS equipped with a 633 nm He–Ne laser. Transmission electron microscopy (TEM) for morphological observation was operated on the Tecnai G220 TEM (FEI company, OH, USA) at an acceleration voltage of 200 kV. The samples were prepared by placing 20 μL of 1 mg/mL micelles on the 200-mech copper grid, followed by air-dry and stain with 2% (w/v) phosphotungstic acid.

2.5. GSH-triggered release of PTX from MeO-PEG_{2k}-SS-PTX micelles

In vitro release profile of PTX from cross-linked micelles as well as uncross-linked micelles was investigated by a dialysis method (MWCO 1000 Da) at 37 °C in two different media, *i.e.* PBS (pH 7.4) only and PBS (pH 7.4) with 10 mM GSH. The initial PTX concentration of micelles was 1 mg/mL. Typically, 1 mL of micelles was precisely injected into dialysis cartridges (Sigma-Aldrich Co., MS, USA) and dialyzed against 100 mL of dissolution medium containing 0.05% Tween-80. The concentration of released PTX at various time points was analyzed by using HPLC (Agilent, MA, USA). The release tests were carried out in triplicate and values presented were the means with standard deviations (M ± SD).

2.6. MTT assay

The *in vitro* cytotoxicity of cross-linked MeO-SS-PTX micelles was studied using MCF-7 cells, A549 cells and BEL-7402 cells by MTT assay [45]. In brief, appropriate of 5×10^3 cells/well in 96-well plates was incubated in 100 μL of RPMI-1640 medium with 10% FBS (37 °C, 5% CO_2) 24 h prior to the treatment. The micelles with the prescribed concentration of PTX (0.156 μM–10 μM) were added, while free PTX was used as positive control. After 48 h incubation, the microplate-680 reader (ThermoFisher Scientific, MA, USA) was conducted to check the optical density (OD) of each sample after the addition of MTT (20 μL, 5 mg/mL) was dissolved in analytical DMSO at 570 nm. Cell viability (%) of tested groups against cells was determined in comparition to the blank controls containing the cells only and the results were shown as the average data $[(OD_{\text{tested}}\text{-}OD_{\text{blank}})/(OD_{\text{positive}}\text{-}OD_{\text{blank}}) \times 100\%]$ of sextuplicate wells.

2.7. Apoptosis analysis

For the analysis of cell apoptosis *in vitro*, representative MCF-7 cells were treated with different formulations of free PTX and micelles (PTX concentration of 2 μM) for 48 h at 37 °C, 5% CO_2 atmosphere. Afterward, 2×10^4 cells were collected and re-suspended in 0.5 mL of binding buffer. Following the instruments of apoptosis detection kit (KeyGEN BioTECH, Nanjing, China), 10 μL PI and 5 μL Annexin V-FITC were added into the cells for 30 min staining in the dark. Finally, flow cytometry (FACScan, BD Accuri, NJ) was used to record the fluorescence of double stained cells and data analysis was operated on FlowJo software (version 7.6, Tree Star, Inc., OR).

2.8. Hemolysis study

Blood compatibility of cross-linked MeO-PEG_{2k}-SS-PTX micelles was evaluated by hemolysis assay, following the procedure as stated as previously published literatures [46]. Human blood was obtained from Department of Blood Transfusion of Affiliated Zhongda Hospital of Southeast University (Nanjing, China). The red blood cells (RBCs) were isolated by centrifugation at 1000 rpm for 30 min and prepared to a final concentration of 2% (v/v) in phosphate solution (PBS, pH 7.4). 100 μL of RBCs suspension was mixed with MeO-PEG_{2k}-SS-PTX micelles at different concentrations for 37 °C, 4 h incubation. After that, the solution was centrifuged at 1000 rpm for 15 min and the collected supernatant was subjected to analysis by a micro-plate reader (ThermoFisher Scientific, MA, USA) at 540 nm. RBCs treated with deionized water (100% hemolysis) and PBS (pH 7.4, 0% hemolysis) were set as positive and negative controls, respectively. Less than 5% of percent hemolysis ratio (HR%) was regarded as nontoxic and HR% was calculated according to the following formula:

$$\mathrm{HR}(\%) = \frac{OD_{sample} - OD_{negative}}{OD_{positive} - OD_{negative}} \times 100$$

OD_{sample} is the optical density of tested samples, while OD_{negative} and OD_{positive} are the negative control and positive control, respectively.

2.9. In vivo pharmacokinetics and biodistribution

Female BALB/c mice (5-week-old, 18–20 g) were injected with

0.1 mL suspension of 4T1 mammary carcinoma cells (1×10^7) in the right axilla subcutaneously. When the tumor size grew to 80–100 mm^3 for two weeks before testing, the mice were randomly divided into Taxol® and cross-linked MeO-PEG_{2k}-SS-PTX micelles groups (n = 3). The aqueous solutions of two formulations were intravenously administrated via tail vein at the dosage of 5 mg PTX/kg. At various time point post-injection, 100 μL of plasma was collected after centrifugation at 3000 rpm for 15 min. Subsequently, methanol (1 mL) for protein precipitation and extraction of PTX was mixed with the plasma and centrifuged at 11,000 rpm for 5 min to obtain the supernatant. An aliquot of 20 μL of Taxol® samples was directly measured by using HPLC (Agilent, MA, USA), while samples of MeO-PEG_{2k}-SS-PTX micelles were checked after treatment with excessive GSH firstly. The amount of PTX in blood was acquired by HPLC, which is according to the standard curve previously analysis of blood samples containing known amounts of free PTX.

To assess the effect of cross-linked MeO-PEG_{2k}-SS-PTX micelles on tissue distribution, 4T1-bearing BALB/c mice were assigned into 2 groups at random and the protocol for administration in tissue distribution study was the same as the above-described pharmacokinetic analysis. At 1 h, 3 h, 6 h and 12 h after post-injection, all mice (n = 4) were scarified and tissues including heart, liver, spleen, lung and kidney were collected. Free PTX was then extracted from the homogenized tissue samples using 2 mL of diethyl ether. After vortexing for 5 min, the organic phase was gathered, air-dried and re-dissolved in methanol for analysis. The drug concentrations were determined using HPLC, and the corresponding PTX concentrations in tissues were calculated accordingly.

3. Statistical analysis

Statistical analysis between different groups was performed by one-way ANOVA analysis using GraphPad Prism software (version 6, GraphPad Software, Inc., CA). All the results were expressed as mean ± S.D. The value of $^*P < 0.05$ considered significant and $^{**}P < 0.01$ highly significant.

4. Results and discussion

4.1. Synthesis and characterizations of micelles

The objective reduction-responsive MeO-PEG_{2k}-SS-PTX prodrug was synthesized by a thiol–disulfide exchange reaction between polymer MeO-PEG_{2k}-DHLA and PTX–SS–Pyr conjugate (Schemes 1 and 2). ^{1}H NMR spectrum of MeO-PEG_{2k}-SS-PTX prodrug successfully displayed with representative signals at 3.62 ppm and 7.0–8.5 ppm in Fig. S3, which are attributable to the methylene protons of PEG and the phenyl protons of PTX, respectively. In addition, the peaks assignable to $–CH_2CH_2–$ linkage were detected from 1.8 to 2.0 ppm, further confirming the conjugation of PEG and PTX–SS–Pyr.

PTX–SS–Pyr compound was readily conjugated into the thiol-functionalized MeO-PEG_{2k}-DHLA at the fixed molar ratio of 4:1 (PTX: Polymer) in a mild condition and the content of PTX was analyzed by HPLC instrument at the wavelength of 227 nm. As examined, the PTX content in MeO-PEG_{2k}-SS-PTX prodrug was up to 26 wt% as well as the conjugation efficiency (CE) 20%. According to the data, approximate one PTX molecule is conjugated in one MeO-PEG_{2k}-DHLA macromolecule (Scheme 2). It was reported that most polymeric prodrugs possess less than 20 wt% drug content, such as PHPMA-peptide-PTX conjugates (5 wt % PTX, PNU166945) used in phase I clinical trials and PHPMA-hydrazide-LEV-PTX (7.6 − 16.3 wt % PTX) [47], for which could avoid the premature burst drug release in blood circulation. Herein, these reduction-responsive MeO-PEG_{2k}-SS-PTX prodrug significantly improved drug loading without drug leakage, exhibiting a great advantage in prodrug-based delivery of chemotherapeutic agents.

With the inherent amphiphilicity of hydrophilic PEG and hydrophobic PTX domains, MeO-PEG_{2k}-SS-PTX prodrug is definitely bound to self-assemble into micelles in aqueous medium (PBS, pH 7.4). The typical solvent exchange method was used to prepare the uncross-linked MeO-PEG_{2k}-SS-PTX micelles with an average hydrodynamic size of 85.62 nm (Fig. S4), following dropwise a DMF dissolution of prodrug into PBS solution (pH 7.4). Moreover, the thiol-containing MeO-PEG_{2k}-SS-PTX micelles (uncross-linked micelles) are able to spontaneously cross-link forming disulfide bond (–SS–) in the presence of air atmosphere. After bubbled with air for 24 h in uncross-linked micelles, the content of disulfide formation was checked by Ellman's test [48], which was quantitated according to a standard curve composed of series of known cysteine concentrations at 412 nm. Similar to our previous report, it was as-expectedly found that > 95% conversion of thiol group (-SH) was achieved, significantly indicating the cross-link based on the disulfide (–SS–) formation (Data not given).

The aggregation behavior of cross-linked MeO-PEG2k–SS–PTX micelles was monitored by using pyrene fluorescence probe technique. Fig. S5 showed the variation of I3/I1 intensity ratio versus the logarithm of concentration (Log C), where CMC was determined as the concentration at the point of intersection. It was found that the CMC value of MeO-PEG2k–SS–PTX micelles was 19.95 μg/mL and such low CMC value suggested that the micelles can be formed under highly dilute condition in PBS (pH 7.4). The resultant cross-linked MeO-PEG_{2k}-SS-PTX micelles were further characterized for size distribution using DLS and for spherical morphology using TEM, respectively. DLS measurements in Fig. 1A revealed that the average diameter of cross-linked micelles in PBS (pH 7.4) was appropriate 87.67 nm with a narrow distribution (PDI: 0.185), that is close to the uncross-linked individual. Besides, to prove the sufficient crosslinking of micelles, the size and size distribution of cross-liked prodrug dissolved in DMSO were further measured by DLS. As shown in Fig. 1B, the hydrodynamic size of cross-linked micelles in DMSO was 92.48 nm with a with a calculated PDI value of 0.205. The results presented are in consistence with the size that dispersed in PBS (pH 7.4), which convincingly verified the nanostructures of MeO-PEG_{2k}-SS-PTX micelles maintains undamaged in organic solvent, due to the core crosslinking. Fig. 1C exhibited the TEM micrograph of cross-linked micelles. Spherical morphology of uniform sizes was observed, thereby confirming the self-assembly of MeO-PEG_{2k}-SS-PTX prodrug in aqueous.

4.2. Stability study of cross-linked micelles

The storage stability of disulfide cross-linked micelles was found to be excellent at 4 °C, showing no significant size change after one month (Fig. S6). After that, *in vitro* stability of the cross-linked micelles was studied against the harsh micelles-destruction conditions in SDS (2.5 mg/mL). As reported previously, SDS, a powerful ionic detergent, could disrupt the nanostructure of polymeric micelles effectively. The micelles (1 mg/mL) were mixed with the SDS solution at the micelle-destruction concentration of 2.5 mg SDS/mL, the stability in particle changes was accordingly monitored at the determined time intervals by DLS. As shown in Fig. 1D, the cross-linked micelles have a stable size in the presence of SDS. On the contrary, the size of the uncross-linked micelles decreased sharply, indicating SDS inducing micelle destruction.

The attractive target of Me^O-PEG_{2k}-SS-PTX prodrug was its intracellular redox-sensitivity designed for solving the problem of slow release of payload drug. It is well-known that the content of intracellular glutathione (GSH, 10 mM) is substantially higher compared with the extracellular level (2 μM) [49,50]. Thus, the reduction-sensitivity of cross-linked micelles was evaluated by recording the size change in response to the 10 mM GSH using DLS. The results are depicted in Fig. 1D and found the immediate decrease of size signal of cross-linked micelles after 20 min, following the addition of 10 mM GSH in medium containing 2.5 mg/mL SDS. The response of cross-linked MeO-PEG_{2k}-SS-PTX micelles to the reductive GSH supportively

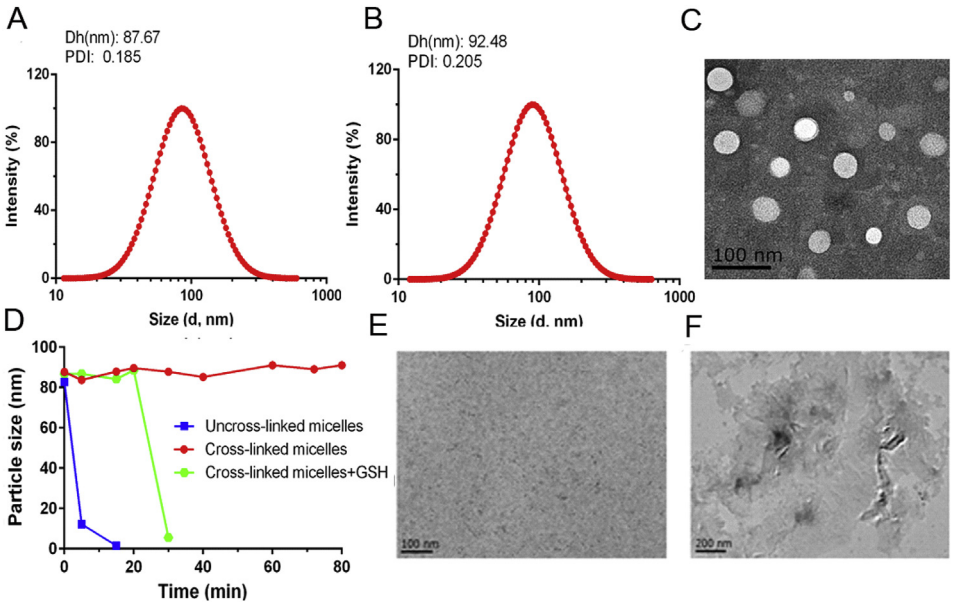

Fig. 1. (A) Size distribution of cross-linked MeO-PEG_{2k}-SS-PTX micelles in PBS (pH 7.4) and (B) in DMSO as determined by DLS. (C) TEM image of cross-linked MeO-PEG_{2k}-SS-PTX micelles after staining with 2% phosphotungstic acid. (D) Stability in particle size of cross-linked and uncross-linked micelles incubated with 2.5 mg/mL SDS. (E) TEM image of the uncross-linked micelles in the presence of 2.5 mg/mL SDS. (F) TEM image of the cross-linked micelles treated with 10 mM GSH in the presence of 2.5 mg/mL SDS.

indicated that a critical number of formed disulfide bonds was cleaved resulting in the rapid destabilization and disruption of the micelles. The morphology of uncross-linked and cross-linked micelles was further observed by TEM in the end of stability study (Fig. 1E and F). It was synergistically confirmed that the nanostructures of uncross-linked micelles were destroyed in ionic detergent of SDS, while cross-linked micelles retained the spherical particles in SDS but completely dissociation in the presence of SDS and GSH.

4.3. Drug release of the micelles

In vitro PTX release from the formulated micelles was investigated by a dialysis method at 37 °C under two stimulated physiological environments: (i) 0.05% Tween/PBS, pH 7.4; (ii) 0.05% Tween/PBS (pH 7.4) + 10 mM GSH. The uncross-linked MeO-PEG_{2k}-SS-PTX micelles were used as a control. As a start, the stability of PTX in PBS containing 0.05% Tween 80 for was monitored to confirm the feasibility of *in vitro* PTX release kinetics. Actually, about 90.3% of PTX was left after 72 h incubation at 37 °C (Fig. S7), indicating its stability in Tween/PBS release medium satisfying long-time sampling. The cumulative release profiles of the micelles was illustrated in Fig. 2. MeO-PEG_{2k}-SS-PTX micelles after crosslinking possessed higher colloidal stability than uncross-lined counterparts in physiological condition (PBS, pH 7.4) with < 15% of cumulative PTX release in 72 h, while the amount of released PTX from uncross-linked micelles was up to 40.3%. The large

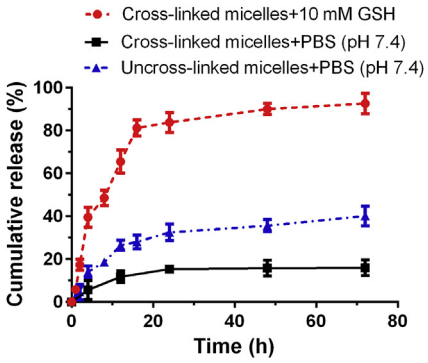

Fig. 2. PTX release profiles of uncross-linked and cross-linked micelles in PBS (pH 7.4) with or without 10 mM GSH at 37 °C. The value is reported as average ± S.D for triplicate samples.

inhibition of release between these two micelles is likely ascribed to the disulfide crosslinking effect, sequestering PTX payload in the hydrophobic cores. As expected, the cross-linked micelles based on the redox-sensitive MeO-PEG_{2k}-SS-PTX prodrug exhibited an obvious GSH-dependant manner of drug release. Appropriate 65.6% of PTX was released from the cross-linked micelles in 12 h and 92.6% in 72 h incubated in PBS medium (pH 7.4, 0.05% Tween 80) containing 10 mM GSH, which is in agreement with the level of intracellular redox microenvironment in tumor cells. These results highlighted that the existence of disulfide (–SS–) linkage in polymeric prodrugs plays a key role in accelerating intracellular drug release. As reported in the literature [51], the release of PTX can be reasonably explained that the cleavage of –SS– bonds in MeO-PEG_{2k}-SS-PTX under the reductive agent GSH generates HS-modificated PTX intermediate (PTX-SH) followed by the reaction of nucleophilic substitution at the carbonate functionality to release free parent PTX with a five-membered ring thiolactone departuring (Scheme 3) as checked by HPLC technique in Fig. S8. Conclusively, the reduction-responsive cross-linked MeO-PEG_{2k}-SS-PTX micelles would undertake an enhanced intracellular PTX release but maintain an inhibited release during circulation in blood, thereby limiting the systemic cytotoxicity.

4.4. Cytotoxicity and apoptosis assay

MTT assay was conducted to examine the *in vitro* cytotoxicity of the cross-linked MeO-PEG_{2k}-DHLA and MeO-PEG_{2k}-SS-PTX micelles against MCF-7, A549 and BEL-7402 cells using free PTX as positive control and the results were shown in Fig. 3A–C, 3G and Fig. S9. After 48 h incubation, these blank MeO-PEG_{2k}-DHLA micelles possessed nontoxic to the tested cell lines (cell viabilities: 92.7%–98.1%) at the concentration from 31.25 μg/mL to 2 mg/mL, indicating their excellent biocompatibility. By contrast, the designed cross-linked MeO-PEG_{2k}-SS-PTX micelles induced favorable antitumor effect against these three tested cells with a dose-dependent proliferation-inhibition manner. Notably, the cell cytotoxicity of the cross-linked micelles was significantly stronger than that of free PTX group, particularly at high concentration (> 2.5 μM, $^*P < 0.05$). It may be ascribed to the quick PTX release from micelles in response to the reduction environment after internalized into tumor cells, while the low solubility of PTX in culture medium also limits the cytotoxicity of free PTX group. IC_{50} (half maximal inhibitory concentration) was further calculated to quantitatively assess their cytotoxicities. As showed in Fig. 3G, the IC_{50} values of the

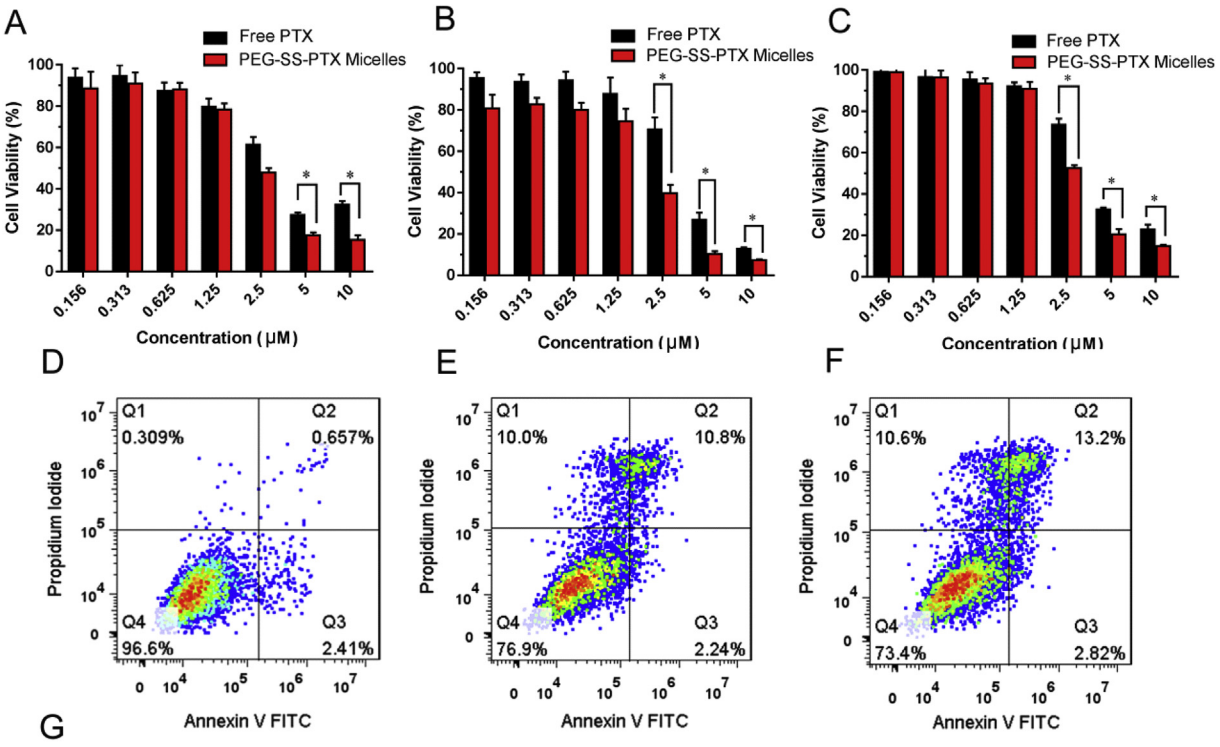

G

Cell Lineage	IC_{50} (μM)		SD (μM)	
	Free PTX	PEG-SS-PTX Micelles	Free PTX	PEG-SS-PTX Micelles
MCF-7	0.403	0.353	0.046	0.069
A549	0.448	0.351	0.026	0.072
BEL-7402	0.474	0.325	0.014	0.077

Fig. 3. *In vitro* cytotoxicity of (A) MCF-7, (B) A549 and (C) BEL-7402 cells after treatments with free PTX and cross-linked micelles for 48 h. Effect of incubation of (E) free PTX and (F) micelles on cell apoptosis of MCF-7 (48 h, PTX concentration of 2 μM) and (D) the untreated cells were used as blank control, determined by flow cytometry. (G) IC_{50} values of free PTX and micelles against the three cancer line. values are reported as average ± S.D for triplicate samples and $^*P < 0.05$ is set as statistical significance.

cross-linked micelles (0.353 ± 0.069 μM for MCF-7 cells, 0.351 ± 0.072 μM for A549 cells and 0.325 ± 0.077 μM for BEL-7402 cells) were lower than those of free PTX (0.403 ± 0.046 μM for MCF-7 cells, 0.448 ± 0.026 μM for A549 cells and 0.474 ± 0.014 μM for BEL-7402 cells), respectively. Furthermore, a mouse mammary carcinoma cell line, 4T1, was used to evaluate the antitumor activity of the MeO-PEG_{2k}-SS-PTX crosslinked micelles. As indicated in Fig. S10, the cross-linked micelles also exhibited higher antitumor activity than that of free PTX. Based on the reduction-sensitive profile above and the cytotoxicity results presented here, MeO-PEG_{2k}-SS-PTX crosslinked micelles could retain the antitumor efficiency of PTX, emphasizing the contribution of GSH-triggered intracellular drug release in tumor cells.

To further investigate the evaluated apoptosis of reduction-sensitive cross-linked micelles towards MCF-7 cells, Annexin V-FITC/PI double staining assay was utilized to measure their apoptosis-inducing capability. Similar results of quantitative analysis in Fig. 3D–F were achieved as the provided MTT assay. The order of apoptosis ratio (AR, Q2 + Q3) was cross-linked MeO-PEG_{2k}-SS-PTX micelles > free PTX. Precisely, the percentage of AR was established to be 16.02% for the micelles while the group of free PTX was 13.04% at the same concentration of 2 μM. The data differences further demonstrated the higher cytotoxicity of the developed micelles.

4.5. Pharmacokinetics and biodistribution

Since nanoparticles were intravenously administrated into blood circulation for drug delivery, destructive interactions between these nanoparticles and blood components must be avoided [52,53]. Herein, *in vitro* hemolysis analysis of MeO-PEG_{2k}-SS-PTX prodrug-based micelles was studied in detail and the degree of hemolysis incubated with 2% human blood for 4 h is illustrated in Fig. S11. As seen, the percentage of hemolysis ratio (HR) slightly increased as a function of increasing mass MeO-PEG_{2k}-SS-PTX concentrations with blood constitutes. But for the overall HR% of each group, percentage less than 5% indicated that the tested nanomaterials are safe for *in vivo* injections without damage to red blood cells (RBCs).

Accordingly, *in vivo* pharmacokinetics of cross-linked MeO-PEG_{2k}-SS-PTX micelles was evaluated by administrating the respective PTX dosage at 5 mg/kg to 4T1-bearing BALB/c mice. Considering that Taxol®, as a clinical case, is formulated with the 1:1 (v/v) mixture of Cremophor EL and dehydrated alcohol for enhancing the solubility of PTX *in vivo*, Taxol® was chosen as the positive control in this content. Fig. 4A shows the plasma concentration−time profiles of two formulations and the corresponding pharmacokinetic parameters were calculated in Table 1. Apparently, MeO-PEG_{2k}-SS-PTX micelles possess an extended blood circulation time compared with Taxol®, with a 1.46-fold longer elimination half-life ($t_{1/2}$), 1.53-fold higher mean residence

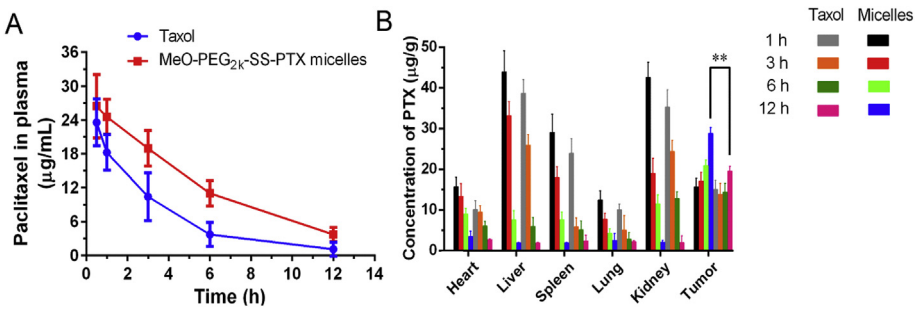

Fig. 4. *In vivo* (A) pharmacokinetic profile and (B) tissue distribution of Taxol® and cross-linked MeO-PEG$_{2k}$-SS-PTX micelles at the equivalent dosage of 5 mg PTX/kg (M ± S. D, n = 3). The statistical significance level is $^{**}P < 0.01$.

Table 1
Pharmacokinetic parameters of Taxol® and cross-linked MeO-PEG$_{2k}$-SS-PTX micelles in 4T1-bearing BALB/c mice after i.v. administration at the equivalent PTX dosage of 5 mg/kg (n = 3).

[a]Parameters (unit)	Taxol®	MeO-PEG$_{2k}$-SS-PTX micelles
AUC_{0-t} (mg/L·h)	80.76	152.17
MRT_{0-inf} (h)	3.69	5.63
$t_{1/2}$ (h)	2.62	3.83
V_z (L/kg)	0.16	0.22
CL (L/h/kg)	0.029	0.006
C_{max} (μg/mL)	23.56	26.46
T_{max}	0.5	0.5

[a] Parameters: AUC, area under the curve from zero to time t; MRT_{0-inf}, residence time; $t_{1/2}$, elimination half-life; CL, plasma clearance; Vz, apparent volume of distribution during elimination phase; C_{max}, peak plasma concentration; T_{max}, peak plasma time.

time (MRT_{0-inf}), 1.88-fold larger area under the curve (AUC_{0-t}) and the decreased value of plasma clearance (CL, 0.006 L/h/kg), which can facilitate the accumulation of payload in micelles to tumor sites. The better performance of MeO-PEG$_{2k}$-SS-PTX micelles *in vivo* might be ascribed to the following several aspects: (i) Nanoscaled character of cross-linked micelles (< 100 nm) allows them significantly circumvent the rapid uptake of reticular endothelial system (RES); (ii) The combination of core crosslinking and surface modified by PEG segment results in the strong stability in physiological environment without disassembly as well as declining plasma elimination. These results were in accordance with previously published data, where a manifold increase in the plasma concentrations was observed after PEGylation.

In order to observe the passive targeting accumulation of cross-linked micelles to 4T1-bearing BALB/c tumors, different tissue biodistribution including tumor, heart, liver, spleen lung and kidney of PTX was investigated at designed time intervals. As shown in Fig. 4B, PTX in cross-linked micelles was rapidly distributed into the majority of tissues after administration through tail vein. The maximum concentration of PTX was recorded in liver, followed the order of kidney and spleen within 1 h post-injection. Although MeO-PEG$_{2k}$-SS-PTX micelles and Taxol® held the similar effect of PTX biodistribution in mice, significant enhanced tumor accumulation of micelles was acquired compared with Taxol®. At 1 h time period, the amount of PTX checked by HPLC was 15.65 μg/g that is approximately equivalent to Taxol® group (15.02 μg/g). Subsequently, its concentration passively targeted in tumor sites was 1.23, 1.45 and 1.47 times higher than that of Taxol® group at 3 h, 6 h and 12 h, respectively. It was supported that the reduction-responsive PEGylated PTX micelles can efficiently inhibit the fast clearance of RES system but passively accumulate in tumor tissue owing to the EPR effects, offering a promising perspective for ideal evaluations of *in vivo* antitumor activity.

5. Conclusion

In summary, a novel disulfide cross-linked micelle based on MeO-PEG$_{2k}$-SS-PTX prodrug was successfully developed, which possess the characteristics of high drug loading efficiency, rapid reduction-sensitive drug release, the EPR-specific PEG detachment, prolonged blood circulation and passively accumulation of PTX to tumors *in vivo*. The results presented here drastically demonstrated these reduction-responsive prodrug micelles via crosslinking are able to maintain the chemotherapic capacity of PTX in delivering system and inhibit tumor cells growth effectively both *in vitro* and *in vivo*. These PTX prodrug micelles show a great potential as versatile platform and may be further studied for combined applications with other drugs or tumor-targeted drug delivery.

Conflicts of interest

We declare that we have no financial and personal relationships with other people or organizations that can inappropriately influence our work, there is no professional or other personal interest of any nature or kind in any product, service and/or company that could be construed as influencing the position presented in, or the review of this paper.

Acknowledgement

This research was supported by the Major National Science and Technology Program for Innovative Drug from the Ministry of Science and Technology of China (2017ZX09101002-001-004).

Appendix A. Supplementary data

Supplementary data to this article can be found online at https://doi.org/10.1016/j.jddst.2019.101168.

References

[1] P. Sapra, T. Allen, Ligand-targeted liposomal anticancer drugs, Prog. Lipid Res. 42 (5) (2003) 439–462.
[2] T. Kubo, T. Sugita, S. Shimose, et al., Targeted delivery of anticancer drugs with intravenously administered magnetic liposomes in osteosarcoma-bearing hamsters, Int. J. Oncol. 17 (2) (2000) 309–324.
[3] H. Cabral, K. Kataoka, Progress of drug-loaded polymeric micelles into clinical studies, J. Control. Release 190 (2014) 465–476.
[4] E. Kadife, E. Chan, R. Luwor, et al., Paclitaxel-induced Src activation is inhibited by dasatinib treatment, independently of cancer stem cell properties, in a mouse model of ovarian cancer, Cancers 11 (2) (2019) 243.
[5] A. Potineni, D.M. Lynn, R. Langer, et al., Poly (ethylene oxide)-modified poly (β-amino ester) nanoparticles as a pH-sensitive biodegradable system for paclitaxel delivery, J. Control. Release 86 (2–3) (2003) 223–234.
[6] A. Dalla Pria, M. Bower, AIDS-related Malignant Disease, (2018) Medicine.
[7] C. Xu, H. Li, K. Zhang, et al., Photo-controlled release of paclitaxel and model drugs from RNA pyramids, Nano Res. 12 (1) (2019) 41–48.
[8] S. Hussain, D.N. Anderson, M.E. Salvatti, et al., Onycholysis as a complication of systemic chemotherapy: report of five cases associated with prolonged weekly

paclitaxel therapy and review of the literature, Cancer 88 (10) (2000) 2367–2371.
[9] A.J. Montero, B. Adams, C.M. Diaz-Montero, et al., Nab-paclitaxel in the treatment of metastatic breast cancer: a comprehensive review, Expert Rev. Clin. Pharmacol. 4 (3) (2011) 329–334.
[10] T.B. Stage, T.K. Bergmann, D.L. Kroetz, Clinical pharmacokinetics of paclitaxel monotherapy: an updated literature review, Clin. Pharmacokinet. 57 (1) (2018) 7–19.
[11] A. Kumar, H. Kaur, A. Singh, Neuropathic Pain models caused by damage to central or peripheral nervous system, Pharmacol. Rep. 70 (2) (2018) 206–216.
[12] C.A. Rabik, M.E. Dolan, Molecular mechanisms of resistance and toxicity associated with platinating agents, Cancer Treat Rev. 33 (1) (2007) 9–23.
[13] W. Xiao, H. Zheng, G. Bennett, Characterization of oxaliplatin-induced chronic painful peripheral neuropathy in the rat and comparison with the neuropathy induced by paclitaxel, Neuroscience 203 (2012) 194–206.
[14] J. Bhattacharyya, J.J. Bellucci, I. Weitzhandler, et al., A paclitaxel-loaded recombinant polypeptide nanoparticle outperforms Abraxane in multiple murine cancer models, Nat. Commun. 6 (2015) 7939.
[15] Q. Chen, C. Liang, C. Wang, et al., An imagable and photothermal “Abraxane-like” nanodrug for combination cancer therapy to treat subcutaneous and metastatic breast tumors, Adv. Mater. 27 (5) (2015) 903–910.
[16] Y. Matsumura, K. Kataoka, Preclinical and clinical studies of anticancer agent-incorporating polymer micelles, Cancer Sci. 100 (4) (2009) 572–579.
[17] J. Nicolas, S. Mura, D. Brambilla, et al., Design, functionalization strategies and biomedical applications of targeted biodegradable/biocompatible polymer-based nanocarriers for drug delivery, Chem. Soc. Rev. 42 (3) (2013) 1147–1235.
[18] J. Thévenot, H. Oliveira, O. Sandre, et al., Magnetic responsive polymer composite materials, Chem. Soc. Rev. 42 (17) (2013) 7099–7116.
[19] A.Z. Wilczewska, K. Niemirowicz, K.H. Markiewicz, et al., Nanoparticles as drug delivery systems, Pharmacol. Rep. 64 (5) (2012) 1020–1037.
[20] T.M. Allen, P.R. Cullis, Drug delivery systems: entering the mainstream, Science 303 (5665) (2004) 1818–1822.
[21] H. Maeda, G. Bharate, J. Daruwalla, Polymeric drugs for efficient tumor-targeted drug delivery based on EPR-effect, Eur. J. Pharm. Biopharm. 71 (3) (2009) 409–419.
[22] A. MaHam, Z. Tang, H. Wu, et al., Protein-based nanomedicine platforms for drug delivery, Small 5 (15) (2009) 1706–1721.
[23] S. Li, X. Wang, W. Li, et al., Preparation and characterization of a novel conformed bipolymer paclitaxel-nanoparticle using tea polysaccharides and zein, Carbohydr. Polym. 146 (2016) 52–57.
[24] Z. Liu, Y. Jiao, Y. Wang, et al., Polysaccharides-based nanoparticles as drug delivery systems, Adv. Drug Deliv. Rev. 60 (15) (2008) 1650–1662.
[25] Y. Bao, Y. Guo, X. Zhuang, et al., D-α-tocopherol polyethylene glycol succinate-based redox-sensitive paclitaxel prodrug for overcoming multidrug resistance in cancer cells, Mol. Pharm. 11 (9) (2014) 3196–3209.
[26] H.-J. Youk, E. Lee, M.-K. Choi, et al., Enhanced anticancer efficacy of α-tocopheryl succinate by conjugation with polyethylene glycol, J. Control. Release 107 (1) (2005) 43–52.
[27] Z. Zhang, S.-S. Feng, The drug encapsulation efficiency, *in vitro* drug release, cellular uptake and cytotoxicity of paclitaxel-loaded poly (lactide)–tocopheryl polyethylene glycol succinate nanoparticles, Biomaterials 27 (21) (2006) 4025–4033.
[28] H.S. Abandansari, M.R. Nabid, S.J.T. Rezaei, et al., pH-sensitive nanogels based on Boltorn® H40 and poly (vinylpyridine) using mini-emulsion polymerization for delivery of hydrophobic anticancer drugs, Polymer 55 (16) (2014) 3579–3590.
[29] M. Agüeros, V. Zabaleta, S. Espuelas, et al., Increased oral bioavailability of paclitaxel by its encapsulation through complex formation with cyclodextrins in poly (anhydride) nanoparticles, J. Control. Release 145 (1) (2010) 2–8.
[30] M. Shah, V. Shah, A. Ghosh, et al., Molecular inclusion complexes of β-cyclodextrin derivatives enhance aqueous solubility and cellular internalization of paclitaxel: preformulation and *in vitro* assessments, J. Pharm. Pharmacol. 2 (2) (2015) 8.
[31] K.L. Aillon, Y. Xie, N. El-Gendy, et al., Effects of nanomaterial physicochemical properties on *in vivo* toxicity, Adv. Drug Deliv. Rev. 61 (6) (2009) 457–466.
[32] L.H. Reddy, J.L. Arias, J. Nicolas, et al., Magnetic nanoparticles: design and characterization, toxicity and biocompatibility, pharmaceutical and biomedical applications, Chem. Rev. 112 (11) (2012) 5818–5878.
[33] A.N. Koo, H.J. Lee, S.E. Kim, et al., Disulfide-cross-linked PEG-poly (amino acid) s copolymer micelles for glutathione-mediated intracellular drug delivery, Chem. Commun. 48 (2008) 6570–6572.
[34] Y. Li, K. Xiao, W. Zhu, et al., Stimuli-responsive cross-linked micelles for on-demand drug delivery against cancers, Adv. Drug Deliv. Rev. 66 (2014) 58–73.
[35] R.K. O'Reilly, C.J. Hawker, K.L. Wooley, Cross-linked block copolymer micelles: functional nanostructures of great potential and versatility, Chem. Soc. Rev. 35 (11) (2006) 1068–1083.
[36] Y. Che, A. Datar, K. Balakrishnan, et al., Ultralong nanobelts self-assembled from an asymmetric perylene tetracarboxylic diimide, J. Am. Chem. Soc. 129 (23) (2007) 7234–7235.
[37] F. Li, Y. Zhu, B. You, et al., Smart hydrogels Co-switched by hydrogen bonds and π–π stacking for continuously regulated controlled-release system, Adv. Funct. Mater. 20 (4) (2010) 669–676.
[38] T. Suzuki, S. Shinkai, K. Sada, Supramolecular crosslinked linear poly (trimethylene iminium trifluorosulfonimide) polymer gels sensitive to light and thermal stimuli, Adv. Mater. 18 (8) (2006) 1043–1046.
[39] M. Talelli, M. Iman, A.K. Varkouhi, et al., Core-crosslinked polymeric micelles with controlled release of covalently entrapped doxorubicin, Biomaterials 31 (30) (2010) 7797–7804.
[40] C.F. Van Nostrum, Covalently cross-linked amphiphilic block copolymer micelles, Soft Matter 7 (7) (2011) 3246–3259.
[41] A.E. Ferentz, G.L. Verdine, Disulfide-crosslinked oligonucleotides, J. Am. Chem. Soc. 113 (10) (1991) 4000–4002.
[42] L. Ling, Y. Du, M. Ismail, et al., Self-assembled liposomes of dual paclitaxel-phospholipid prodrug for anticancer therapy, Int. J. Pharm. 526 (1–2) (2017) 11–22.
[43] X. Zhang, K. Liu, Y. Huang, et al., Reduction-sensitive dual functional nanomicelles for improved delivery of paclitaxel, Bioconjug. Chem. 25 (9) (2014) 1689–1696.
[44] D. Fischer, Y. Li, B. Ahlemeyer, et al., *In vitro* cytotoxicity testing of polycations: influence of polymer structure on cell viability and hemolysis, Biomaterials 24 (7) (2003) 1121–1131.
[45] G. Lv, D. Sun, J. Zhang, et al., Lx2-32c, a novel semi-synthetic taxane, exerts antitumor activity against prostate cancer cells *in vitro* and *in vivo*, Acta Pharm. Sin. B 7 (1) (2017) 52–58.
[46] N. Murthy, I. Chang, P. Stayton, et al., pH-sensitive hemolysis by random copolymers of alkyl acrylates and acrylic acid, Proceedings of the Macromolecular Symposia, Wiley Online Library, 2001F.
[47] Y. Gu, Y. Zhong, F. Meng, et al., Acetal-linked paclitaxel prodrug micellar nanoparticles as a versatile and potent platform for cancer therapy, Biomacromolecules 14 (8) (2013) 2772–2780.
[48] M. Moser, T. Behnke, C. Hamers-Allin, et al., Quantification of PEG-maleimide ligands and coupling efficiencies on nanoparticles with Ellman's reagent, Anal. Chem. 87 (18) (2015) 9376–9383.
[49] B.L. Hogan, E.S. Yeung, Determination of intracellular species at the level of a single erythrocyte via capillary electrophoresis with direct and indirect fluorescence detection, Anal. Chem. 64 (22) (1992) 2841–2845.
[50] L. Yan, W. Wu, W. Zhao, et al., Reduction-sensitive core-cross-linked mPEG–poly (ester-carbonate) micelles for glutathione-triggered intracellular drug release, Polym. Chem. 3 (9) (2012) 2403–2412.
[51] X. Hu, J. Hu, J. Tian, et al., Polyprodrug amphiphiles: hierarchical assemblies for shape-regulated cellular internalization, trafficking, and drug delivery, J. Am. Chem. Soc. 135 (46) (2013) 17617–17629.
[52] P. Aggarwal, J.B. Hall, C.B. McLeland, et al., Nanoparticle interaction with plasma proteins as it relates to particle biodistribution, biocompatibility and therapeutic efficacy, Adv. Drug Deliv. Rev. 61 (6) (2009) 428–437.
[53] Y. Yang, D. Guan, L. Lei, et al., H6, a novel hederagenin derivative, reverses multidrug resistance *in vitro* and *in vivo*, Toxicol. Appl. Pharmacol. 341 (2018) 98–105.